

# SUSY CONTRIBUTIONS TO $R_b$ AND TOP QUARK DECAY

Manuel Drees<sup>1</sup>, R.M. Godbole<sup>2</sup>, Monoranjan Guchait<sup>3</sup>,  
Sreerup Raychaudhuri<sup>3</sup> and D.P. Roy<sup>3</sup>

<sup>1</sup>Physics Dept., University of Wisconsin, Madison, WI 53706, USA.

<sup>2</sup>Centre for Theoretical Studies, Indian Inst. of Science, Bangalore 560 012, India  
(on leave of absence from the Department of Physics, University of Bombay, Mumbai, India.

<sup>3</sup>Theoretical Physics Group, Tata Inst. of Fundamental Research,  
Mumbai 400 005, India.

## Abstract

Stop contributions to radiative corrections to  $R_b$  and the top quark decay are analysed over the relevant MSSM parameter space. One sees a 30% increase in the former along with a similar drop in the latter in going from the higgsino dominated to the mixed region. Consequently one can get a viable SUSY contribution to  $R_b$  within the constraint of the top quark data only in the mixed region, corresponding to a photino dominated LSP. We discuss the phenomenological implications of this model for top quark decay and direct stop production, which can be tested with the Tevatron data.

Pacs Nos: 12.15.Lk, 14.65.Ha, 14.80.Ly

# 1. INTRODUCTION

One of the most intriguing results from the precision measurement of  $Z$  boson parameters at LEP is the  $R_b$  anomaly i.e. the ratio

$$R_b = \Gamma_Z^{\bar{b}b} / \Gamma_Z^{\text{had}} \quad (1)$$

is observed to be about  $3\sigma$  higher than the standard model (SM) prediction. This has aroused a good deal of theoretical interest for two reasons. Firstly, there is a natural source for a significant contribution to this quantity from the minimal supersymmetric extension of the standard model (MSSM) [1], due to the large top quark mass. Secondly, such a contribution would reduce the SM contribution to  $\Gamma_Z^{\text{had}}$  slightly and bring the resulting  $\alpha_s(M_Z)$  in better agreement with its global average value [2] of

$$\alpha_s(M_Z) = .117 \pm .005. \quad (2)$$

It should be mentioned here that the measured value of  $R_c$  seems to be  $1.7\sigma$  below the SM prediction. But there is no natural theoretical source for this deficit. One can accommodate this by invoking extra fermions [3] or an extra  $Z$  boson [4]. But then one has to assume an exact cancellation between their contributions to  $R_q$  ( $q = u, d, s, c, b$ ) in order to preserve the agreement of the extremely precise measurement of  $\Gamma_Z^{\text{had}}$  with its SM prediction. Thus it is fair to surmise that the  $R_c$  anomaly does not have the same experimental or theoretical significance as  $R_b$ . Following the standard practice, we shall explore the  $R_b$  anomaly by assuming  $R_c$  to be equal to its SM value of 0.172. With this assumption, the current experimental value of  $R_b$  is [5]

$$R_b^{\text{exp}} = 0.2202 \pm 0.0016, \quad (3)$$

which is  $2.8\sigma$  above the SM value of

$$R_b^{\text{SM}} = 0.2157(0.2158) \text{ for } m_t = 175(170)\text{GeV}. \quad (4)$$

There are two MSSM solutions to the  $R_b$  anomaly corresponding to the two distinct regions,  $\tan\beta \simeq 1$  and  $\sim m_t/m_b$ , where  $\tan\beta$  is the ratio of the two higgs vacuum expectation values. The relevant MSSM contribution comes from the radiative correction involving stop-chargino exchanges in the first case, while the dominant contribution comes from the higgs exchange in the second case [6, 7, 8]. Correspondingly one expects a significant contribution to top quark decay from the stop-neutralino and charged higgs channels respectively. In the present work we shall be concentrating in the first case, i.e.,  $\tan\beta \simeq 1$ .

Admittedly there is a vast literature analysing the MSSM contribution to  $R_b$  in the low  $\tan\beta$  region [7]. However, there is as yet no systematic exploration of the MSSM parameter space to obtain the best solution to the  $R_b$  anomaly, while taking account of the constraint from top quark decay simultaneously. The present work is devoted to this exercise. In particular we shall see that, contrary to the popular notion, there is no viable solution to the  $R_b$  anomaly from the higgsino dominated region, once the top decay constraint is taken into account. With this constraint, by far the best solution comes from the mixed region, corresponding to a photino dominated LSP.

In the following section we briefly discuss the MSSM formalism along with the relevant formulae for SUSY contributions to  $R_b$  as well as top quark decay. In the next section we shall present our results for SUSY contributions to  $R_b$  and the top branching ratio over a wide range of the MSSM parameters and identify the region that gives the best solution to the  $R_b$  anomaly within the constraints from top quark decay. We shall also discuss the phenomenological implication of this model for top quark decay and direct stop production, which can be tested with Tevatron data. We shall conclude with a summary of our results.

## 2. FORMALISM :

If squarks are degenerate at the Planck or GUT scale, the large top quark mass implies the following mass hierarchy among the right and left handed stops and the remaining squarks at the weak scale,

$$m_{\tilde{t}_R} < m_{\tilde{t}_L} < m_{\tilde{q}}. \quad (5)$$

After mixing the lighter stop

$$\tilde{t}_1 = \cos \theta_{\tilde{t}} \tilde{t}_R - \sin \theta_{\tilde{t}} \tilde{t}_L \quad (6)$$

can have a significantly smaller mass than the other squarks. We shall be primarily interested in this stop, which is expected to have a dominant  $\tilde{t}_R$  component.

We assume that the soft masses of the  $SU(2) \times U(1) \times SU(3)$  gauginos are related via the GUT relations,

$$M_1 = \frac{5}{3} \tan^2 \theta_W M_2 \simeq 0.5 M_2. \quad (7)$$

$$M_3 = \frac{\alpha_S}{\alpha} \sin^2 \theta_W M_2 \simeq 3.5 M_2. \quad (8)$$

Thus all the gaugino masses are given in terms of a single mass parameter  $M_2$ , while the higgsino masses are controlled by the supersymmetric mass parameter  $\mu$  [1]. The  $SU(2)$  and  $U(1)$  gauginos mix with the two higgsino to form the physical neutralino ( $\tilde{Z}_i$ ) and chargino ( $\tilde{W}_i$ ) states, i.e.,

$$\tilde{Z}_i = N_{i1} \tilde{B} + N_{i2} \tilde{W}^3 + N_{i3} \tilde{H}_1^0 + N_{i4} \tilde{H}_2^0, \quad (9)$$

$$\tilde{W}_{iL} = V_{i1} \tilde{W}_L^\pm + V_{i2} \tilde{H}_L^\pm, \tilde{W}_{iR} = U_{i1} \tilde{W}_R^\pm + U_{i2} \tilde{H}_R^\pm. \quad (10)$$

The masses and compositions of the chargino and neutralino states are determined by the three MSSM parameters –  $M_2$ ,  $\mu$  and  $\tan \beta$ . The lightest neutralino  $\tilde{Z}_1$  is assumed to be the lightest superparticle (LSP).

The SUSY contribution to  $R_b$  can be written as [6]

$$\delta R_b = R_b^{\text{SM}}(0) \left[ 1 - R_b^{\text{SM}}(0) \right] \left[ \nabla_b^{\text{SUSY}}(m_t) - \nabla_b^{\text{SUSY}}(0) \right], \quad (11)$$

where  $R_b^{\text{SM}}(0) = 0.2196$  represents the SM value at  $m_t = 0$ .

$$\nabla_b^{\text{SUSY}}(m_t) = \frac{\alpha}{2\pi \sin^2 \theta_W} \cdot \frac{v_L F_L + v_R F_R}{v_L^2 + v_R^2},$$

$$v_L = -\frac{1}{2} + \frac{1}{3} \sin^2 \theta_W, \quad v_R = \frac{1}{3} \sin^2 \theta_W \quad (12)$$

The SUSY contributions to  $Z \rightarrow \bar{b}b$  come from the triangle diagrams involving  $\tilde{W}_i \tilde{W}_j \tilde{t}_k$  and  $\tilde{t}_i \tilde{t}_j \tilde{W}_k$  exchanges as well as the  $\tilde{t}_i \tilde{W}_j$  loop insertions in the  $b$  and  $\bar{b}$  legs. The relevant formulae can be found in [6]. We shall only state them for the  $\tilde{W}_i \tilde{W}_j \tilde{t}_k$  contribution, in a form more convenient for our discussion.

$$F_{L,R} = \sum_{i,j,k} \left[ O_{ij}^{L,R} M_{\tilde{W}_i} M_{\tilde{W}_j} C_0 + O_{ij}^{R,L} \left\{ -M_Z^2 (C_{23} + C_{12}) - \frac{1}{2} + 2C_{24} \right\} \right] \Lambda_{ki}^{L,R} \Lambda_{kj}^{*,L,R} \quad (13)$$

$$\Lambda_{1i}^L = V_{i1}^* \sin \theta_{\tilde{t}} - \frac{m_t}{\sqrt{2} M_W \sin \beta} V_{i2}^* \cos \theta_{\tilde{t}}, \quad \Lambda_{1i}^R = \frac{-m_b}{\sqrt{2} M_W \cos \beta} U_{i2} \sin \theta_{\tilde{t}}, \quad (14)$$

$$O_{ij}^L = -\frac{1}{2} [\cos 2\theta_W \delta_{ij} + U_{i1}^* U_{j1}], \quad O_{ij}^R = -\frac{1}{2} [\cos 2\theta_W \delta_{ij} + V_{i1}^* V_{j1}], \quad (15)$$

where the  $C$  functions are the conventional Passarino–Veltman functions with arguments  $(M_{\tilde{W}_i}, m_{\tilde{t}_k}, M_{\tilde{W}_j})$  [9]. The  $\Lambda_{1i}^{L,R}$  represent the  $b\tilde{t}_1\tilde{W}_i$  couplings, which are common to the other SUSY diagrams. The dominant contribution to (14) comes from the  $b_L\tilde{t}_{1R}\tilde{W}_1$  Yukawa coupling which favours low  $\tan \beta$  ( $\simeq 1$ ) and large  $V_{12}$  – i.e. the higgsino dominated region. On the other hand  $O_{ij}^{L,R}$  represent the  $Z\tilde{W}_i\tilde{W}_j$  couplings. The analogous factor for the  $\tilde{t}_1\tilde{t}_1\tilde{W}_k$  contributions corresponds to the  $U(1)$  coupling of  $Z$  to  $\tilde{t}_{1R}$ , which is relatively small ( $\sim \sin^2 \theta_W$ ). It is evident from Eq. (15) that large  $O_{11}^{L,R}$  favour large  $U_{11}, V_{11}$  – i.e. large gauge components of  $\tilde{W}_1$  [8]. Thus the combined requirements of large  $\Lambda$  and  $O$  couplings favour a  $\tilde{W}_1$  having large higgsino component in  $V(V_{12})$  and gaugino component in  $U(U_{11})$  and/or comparable  $\tilde{W}_1$  and  $\tilde{W}_2$  masses. As pointed out in [8], these conditions cannot be satisfied for  $\mu > 0$ . Consequently the best values of  $\delta R_b$  for positive  $\mu$  are about half of those for negative  $\mu$ . Therefore we shall concentrate on the latter case. In this case the above conditions favour the mixed region ( $|\mu| \sim M_2$ ) over the higgsino dominated one ( $|\mu| \ll M_2$ ). Indeed we shall see that one gets typically 30% larger values of  $\delta R_b$  in the former region compared to the latter.

One has to assume  $\tilde{W}_1, \tilde{t}_1$  masses as well as  $\tan \beta$  close to their lower limits in order to obtain significant values of  $\delta R_b$ . Under these assumptions one predicts a significant SUSY contribution to top decay from  $t \rightarrow \tilde{t}_1 \tilde{Z}_i$ . The relevant formalism has been discussed in [8, 10]. We shall only state the final result.

$$\Gamma(t \rightarrow \tilde{t}_1 \tilde{Z}_i) = \frac{\alpha m_t}{16 \sin^2 \theta_W} \sqrt{1 - 2(x + y_i) + (x - y_i)^2} \left[ (|C_L^i|^2 + |C_R^i|^2) (1 - x + y_i) + 4\sigma_i \text{Re} (C_L^{i*} C_R^i) \sqrt{y_i} \right], \quad (16)$$

where  $x = m_{\tilde{t}_1}^2 / m_t^2$ ,  $y_i = M_{\tilde{Z}_i}^2 / m_t^2$ ,  $\sigma_i = \text{sgn}(M_{\tilde{Z}_i})$  and

$$C_L^i = \left( \frac{1}{3} \tan \theta_W N_{i1} + N_{i2} \right) \sin \theta_{\tilde{t}} + \frac{m_t}{M_W \sin \beta} N_{i4} \cos \theta_{\tilde{t}},$$

$$C_R^i = -\frac{4}{3} \tan \theta_W N_{i1} \cos \theta_t + \frac{m_t}{M_W \sin \beta} N_{i4} \sin \theta_t, \quad (17)$$

represent the  $t\tilde{t}_1\tilde{Z}_i$  couplings (compare Eq. 14). The dominant contributions come from the  $t_L\tilde{t}_{1R}\tilde{N}_i$  and  $t_R\tilde{t}_{1L}\tilde{N}_i$  Yukawa couplings represented by the last terms in  $C_{L,R}^i$ . Thus the favoured decay channel corresponds to the neutralino  $\tilde{Z}_i$  having large  $\tilde{H}_2^0$  component ( $N_{i4}$ ). For the mixed region it corresponds to  $\tilde{Z}_2$ , while the LSP ( $\tilde{Z}_1$ ) is dominantly a photino. But for the higgsino dominated region both  $\tilde{Z}_1$  and  $\tilde{Z}_2$  have large  $\tilde{H}_2$  components. The large phase space available for  $t \rightarrow \tilde{t}_1\tilde{Z}_1$  makes it the dominant decay mode for this region, while  $t \rightarrow \tilde{t}_1\tilde{Z}_2$  is the dominant one in the mixed region. Moreover, the overall SUSY branching ratio ( $B_S$ ) for top is significantly larger in the former case. Consequently the higgsino dominated region is more vulnerable to the constraints on  $B_S$  from the top quark decay experiments [11, 12].

### 3. RESULTS AND DISCUSSION :

It is well known that one cannot get as large a SUSY contribution to  $R_b$  ( $= .0045$ ) as required by the central value of the data (3). We shall consider a contribution of about half this value, i.e.

$$\delta R_b = .0018 - .0026, \quad (18)$$

as viable. It would bring  $R_b$  to within  $1.6\sigma$  of the data (i.e. the 90% CL limit). Moreover since  $\Delta\alpha_s \simeq -4\delta R_b$ , it will exactly bridge the gap between  $\alpha_s \simeq 0.124 \pm .007$  [2] as measured from the  $\Gamma_Z^{\text{had}}$  and its global average value (2). The upper limit on the SUSY branching fraction of top decay is usually assumed to be

$$B_S < 0.4, \quad (19)$$

from the top decay data [7, 13]. The quantitative basis of this assumption will be discussed later.

Although we shall make a detailed scan of the parameter space, it will be useful to focus on three representative points in the  $(M_2, \mu)$  plane,

$$A. (150, -40) \text{ GeV}, \quad B. (60, -60) \text{ GeV}, \quad C. (40, -70) \text{ GeV}, \quad (20)$$

where  $A$  belongs to the higgsino dominated region and  $B, C$  to the mixed region. They have been chosen to give the most favourable values of  $\delta R_b$  in their respective regions, within the allowed parameter space. Table I shows the corresponding chargino and neutralino masses and compositions for  $\tan \beta = 1.1$ , which is close to its lower limit of 1 [1].

For  $A$ , the  $\tilde{W}_1$  mass of 70 GeV is very close to the LEP-1.5 limit of 65 GeV [14]. The  $\tilde{W}_1$  is higgsino dominated in both its  $U$  and  $V$  components, and so are the two lightest neutralinos  $\tilde{Z}_{1,2}$ . The former implies small  $Z\tilde{W}_1\tilde{W}_1$  couplings (15) and hence a modest  $\delta R_b$  despite the low  $\tilde{W}_1$  mass. The latter implies large  $t \rightarrow \tilde{t}_1\tilde{Z}_{1,2}$  branching ratio ( $B_S$ ), in potential conflict with the top decay constraint (19). For  $B$  and  $C$ , on the other hand, the charginos are roughly degenerate and  $\tilde{W}_2$  has a large gaugino (higgsino) component in  $U(V)$ . This implies large  $Z\tilde{W}\tilde{W}$  couplings (15) and hence a more favourable  $\delta R_b$  despite the larger chargino mass. Among the lighter neutralinos only  $\tilde{Z}_2$  has a large  $\tilde{H}_2$  component, while the  $\tilde{Z}_1$  is

completely gaugino dominated [15]. This implies a comparatively smaller SUSY branching ratio ( $B_S$ ) for top decay. As we shall see below, the point  $C$  gives far the best  $R_b$  and least  $B_S$ , as desired. However, it is very close to the MSSM limit of

$$M_2 > 36 \text{ GeV}, \quad (21)$$

corresponding to a gluino mass limit of  $m_{\tilde{g}} > 150 \text{ GeV}$  [16] via eq. (8) [17]. In other words  $M_2 = 40 \text{ GeV}$  implies a gluino mass  $m_{\tilde{g}} = 160 \text{ GeV}$  only. Note that the corresponding gluino mass for  $M_2 = 60 \text{ GeV}$  is  $240 \text{ GeV}$ . Thus both the chargino and gluino masses corresponding to the point  $B$  are safely above the reach of LEP-2 and Tevatron respectively. What constrains this point is the LEP-1 limit,  $M_{\tilde{Z}_1} + M_{\tilde{Z}_2} \gtrsim M_Z$ , which is not going to get any stronger.

The stop mass has the usual LEP bound [2],  $m_{\tilde{t}_1} > 45 \text{ GeV}$ . There is also a constraint from the  $D\bar{D}$  experiment [18], i.e.

$$m_{\tilde{t}_1} \neq 65 - 88 \text{ GeV for } M_{\tilde{Z}_1} \leq 35 \text{ GeV}. \quad (22)$$

It is based on the neutral current decay mode

$$\tilde{t}_1 \rightarrow c\tilde{Z}_1, \quad (23)$$

assuming  $m_{\tilde{t}_1} < M_{\tilde{W}_1} + m_b$ . Thus it applies to  $B$  and  $C$ , but not for the higgsino dominated case  $A$ .

### SUSY contributions to $R_b$ and top $BR$ :

Fig. 1 shows the SUSY contributions to  $R_b$  and the top  $BR$  as functions of the stop mixing angle  $\theta_{\tilde{t}}$  and the lighter stop mass  $m_{\tilde{t}_1}$ . The three parts of the figure (a,b,c) correspond to the three cases  $A, B, C$  respectively. The SUSY  $R_b$  ( $\delta R_b$ ) is clearly seen to peak at small negative value of  $\theta_{\tilde{t}}$  ( $\simeq -5^\circ$ ) as expected from (13,14). On the other hand the SUSY  $BR$  ( $B_S$ ) curves peak at large positive values of  $\theta_{\tilde{t}}$  as per (16,17). Its insensitivity to  $\theta_{\tilde{t}}$  for the case  $A$  is due to the fact that both the higgsino dominated neutralinos are kinematically accessible in this case to top quark decay. The range  $-15^\circ \leq \theta_{\tilde{t}} \leq 0$  represents an optimal range for getting a large  $\delta R_b$  along with a modest  $B_S$ .

The numerical values of these quantities show a striking difference between the higgsino dominated case (A) and the mixed cases (B,C). In the former case (Fig. 1a) the SUSY  $BR$  ( $B_S$ ) is generally larger than the Tevatron constraint (19). One gets a  $B_S$  of .46 for  $m_{\tilde{t}_1} \simeq 80 \text{ GeV}$  and  $\theta_{\tilde{t}} \simeq -15^\circ$ , corresponding to  $\delta R_b = .0014$ . One can of course suppress  $B_S$  by going to a higher  $m_{\tilde{t}_1}$  along with a lower  $|\theta_{\tilde{t}}|$  [19]. It is clear however that one cannot get any significant enhancement of  $\delta R_b$ . Thus the higgsino dominated region cannot give a  $\delta R_b$  in the required range of (18) within the top decay constraint (19). In contrast the mixed case  $B$  (Fig. 1b) gives  $\delta R_b = .0018 - .0022$  with  $B_S = 0.3 - 0.4$  for  $m_{\tilde{t}_1} = 70 - 60 \text{ GeV}$  and  $\theta_{\tilde{t}} \simeq -15^\circ$ . The mixed case  $C$  (Fig. 1c) gives even a better  $\delta R_b = .0020 - .0024$  with  $B_S = 0.3 - 0.4$  for  $m_{\tilde{t}_1} = 70 - 50 \text{ GeV}$  and  $\theta_{\tilde{t}} \simeq -15^\circ$ . Thus in the mixed region one can get a significant  $\delta R_b$  in the range (18) within the top decay constraint on  $B_S$  (19). Note that one could trade off a lower value of  $|\theta_{\tilde{t}}|$  for a higher stop mass without changing  $\delta R_b$  and  $B_S$ .

Similarly one can trade off a higher  $\tan\beta$  for a lower stop mass, as we shall see below. This will be useful for keeping the stop mass within the  $D\emptyset$  constraint (22) [18].

Fig. 2 shows the SUSY contributions to  $R_b$  ( $\delta R_b$ ) and top  $BR(B_S)$  as contour plots in the  $M_2, \mu$  plane for,  $\theta_{\tilde{t}} = -15^\circ$ ,  $\tan\beta = 1.1$  and stop masses of 50 and 60  $GeV$ , which are below the  $D\emptyset$  excluded region (22). The region excluded by LEP-1 and LEP-1.5 ( $M_{\tilde{W}_1} > 65 GeV$ ) are indicated. One gets the best value of  $\delta R_b$  close to the boundary of this region as expected. Much of the remainder is excluded however by the condition  $m_{\tilde{t}_1} > M_{\tilde{Z}_1}$ . One sees a steady increase of  $\delta R_b$  and decrease of  $B_S$  as one moves down from the higgsino dominated region to the mixed one by decreasing the ratio  $M_2/|\mu|$ . The three points  $A, B$  and  $C$  of (20) are indicated by dots. One sees a 30% increase in  $\delta R_b$  along with a similar drop in  $B_S$  as one moves down from the higgsino dominated point ( $A$ ) to the mixed ones ( $B, C$ ). By far the best values of  $\delta R_b$  and  $B_S$  are obtained for the last point  $C$ ; but it is close to the gluino mass limit (21), represented by the  $x$ -axis. Finally one sees a 10% (20%) drop in  $\delta R_b$  ( $B_S$ ) by increasing the stop mass from 50 to 60  $GeV$ .

Fig. 3 shows the analogous contour plots of  $\delta R_b$  and  $B_S$  for  $\tan\beta = 1.4$ . In going from  $\tan\beta = 1.1$  to 1.4 one sees only a 15% drop in  $\delta R_b$  and  $B_S$ . This is because the decrease of  $1/\sin^2\beta$  in (13,14) and (16,17) are partly offset by the drop in the  $\tilde{W}_1$  and  $\tilde{Z}_{1,2}$  masses. Increasing  $\tan\beta$  to 1.6 would result in a further drop of only 5% in these quantities. However the drop in  $\tilde{Z}_{1,2}$  mass brings these points right on to the LEP boundary line.

Table II lists the values of  $\delta R_b$  and  $B_S$  for the mixed cases  $B$  and  $C$  of Figs. 2 and 3. The values lying within the range of (18) and (19) are ticked as viable solutions. Most of the viable solutions correspond to the case  $C$ . Note however that there is one viable solution for the point  $B$  with  $\tan\beta = 1.4$  and a stop mass of 60  $GeV$ . It is an important point as it is not very close to the lower limits of the relevant SUSY masses and  $\tan\beta$ . This is essentially the same as the solution advocated in [8].

Table II also shows that the point  $C$  can give viable solutions for stop masses of 90 – 100  $GeV$ , which lie above the  $D\emptyset$  excluded region (22). This is an interesting case, where one expects charged current decay of stop,

$$\tilde{t}_1 \rightarrow b\tilde{W}_1, \tilde{W}_1 \rightarrow \tilde{Z}_1\ell\nu(qq'). \quad (24)$$

Its phenomenological implications will be discussed at the end of this section.

### Impact on Top Quark Phenomenology:

We shall discuss the phenomenological impact of SUSY decay on the Tevatron top quark events, concentrating on the stop mass range of 50–60  $GeV$ . In this case the viable solutions to  $\delta R_b$  correspond to a

$$B_S = 0.3 - 0.4. \quad (25)$$

The most important sample of top events comes from the isolated lepton plus multijet events with at least 1  $b$ -tag, which satisfy a lepton and a missing  $E_T$  cut of  $E_T^\ell > 20 GeV$  and  $\cancel{E}_T > 20 GeV$  [11, 21]. For the SUSY contribution, one of the top quarks decays into

$$t \rightarrow \tilde{t}_1\tilde{Z}_i, \tilde{t}_1 \rightarrow c\tilde{Z}_1, \quad (26)$$

while the other undergoes SM decay

$$\bar{t} \rightarrow \bar{b}W, \quad W \rightarrow \ell\nu. \quad (27)$$

The dominant  $\tilde{Z}_i$  in the SUSY decay is  $\tilde{Z}_1$  ( $\tilde{Z}_2$ ) for the higgsino dominated (mixed) region. Thus the total number of events will be suppressed by a factor

$$(1 - B_S)^2 + B_S(1 - B_S) \frac{3}{4} \cdot \frac{\epsilon(\cancel{E}_T)}{1 - \epsilon_b/2}, \quad (28)$$

where the two terms represent the SM and SUSY contributions. Here  $\epsilon_b$  is the  $b$ -tagging efficiency and  $\epsilon(\cancel{E}_T)$  represents the efficiency of satisfying the  $\cancel{E}_T > 20 \text{ GeV}$  cut for the SUSY contribution relative to the SM. Substituting the experimental value for  $\epsilon_b \simeq 0.24$  [11, 21] with our estimate of  $\epsilon(\cancel{E}_T) \simeq 1.06$ , the above factor can be approximated by

$$(1 - B_S)^2 + B_S(1 - B_S). \quad (29)$$

Thus the fraction of SUSY contribution to these  $t\bar{t}$  events is  $\simeq B_S$ .

In order to proceed further we have to consider the distribution in the number of jets ( $\sigma_n$ ). As per the CDF jet algorithm the  $E_T^{\text{jet}}$  is obtained by combining all the hadronic  $E_T$  within an angular radius of 0.7 in the  $\eta, \phi$  plane; and all the jets with  $E_T^{\text{jet}} > 15 \text{ GeV}$  coming within the rapidity range  $|\eta_{\text{jet}}| < 2$  are counted. We shall follow a poor man's prescription of incorporating the effects of hadronisation and QCD radiation in a parton level Monte Carlo program by increasing the  $E_T^{\text{jet}}$  threshold from 15 to 20  $\text{GeV}$  and transferring 30% of  $\sigma_n$  to  $\sigma_{n+1}$  [22]. This prescription seems to give reasonable agreement with ISAJET results. It should be adequate for our purpose, which is to estimate the difference between the  $\sigma_n$  distributions of the SM and the SUSY contributions.

Table III shows the fractional  $\sigma_n$  distribution of the SM along with the SUSY contributions for the mixed and the higgsino dominated cases. The SUSY contributions are seen to favour fewer number of jets compared to the SM. This is very pronounced for the higgsino dominated region due to the large  $t \rightarrow \tilde{t}_1 \tilde{Z}_1$  contribution. But even for the mixed region of our interest there is a clear preference for fewer jets compared to the SM. This has several implications for top quark phenomenology, as we see below.

- i) Compared to the SM expectation of 10% of the  $t\bar{t}$  events in the 2-jet channel, one expects an additional contribution of

$$(.35 - .10)B_S = .25B_S, \quad (30)$$

i.e. 7.5 to 10% using (25). The 4th column shows 6.4 expected  $t\bar{t}$  events in the SM from the CDF MC [11], which we expect to include 1 – 2 from the  $\ell\ell$  and  $\ell\tau$  channels of  $t\bar{t}$  decay. Correspondingly we expect  $\sim 4$  more 2-jet events from (25 – 30). This will evidently be favoured by the central value of the data shown in the last column, though the errors are too large to draw any definite conclusion. Similarly one expects a deficit of  $\sim 4$  events in the  $\geq 4$  jet, which is also compatible with data.



- ii) The CDF  $t\bar{t}$  cross-section is based on the sample of  $\geq 3$  jet events. Correspondingly the suppression factor (29) becomes

$$(1 - B_S)^2 + \epsilon_3 B_S(1 - B_S), \quad (31)$$

where  $\epsilon_3$  represents the efficiency of surviving the  $\geq 3$  jet cut for the SUSY contribution relative to the SM. We see from Table III that  $\epsilon_3 = 2/3$  ( $1/4$ ) for the mixed (higgsino dominated) region. Thus the mixed region of our interest corresponds to a suppression factor of

$$(1 - B_S)(1 - B_S + 2B_S/3) = 2/3 - 1/2, \quad (32)$$

for  $B_S = 0.3 - 0.4$ . Therefore the CDF  $t\bar{t}$  cross-section should be compatible with  $2/3$  to  $1/2$  times the QCD value. From the CDF data [11],

$$\sigma_t = 7.5 \pm 1.8 \text{ pb}, \quad m_t = 175.6 \pm 9 \text{ GeV}, \quad (33)$$

it is evident that the central value of their cross-section is already higher than QCD estimate of  $\sigma_t(175) = 5.5 \text{ pb}$  [23]. However taking a  $1.64\sigma$  (90% CL) lower limit on both the quantities would correspond to a  $\sigma_t$  of  $4.5 \text{ pb}$  to be compared with a QCD estimate of  $\sigma_t(160) = 9 \text{ pb}$  [23]. Thus a SUSY BR of 0.4 and  $\epsilon_3 = 2/3$  is barely compatible with the CDF data [24]. The corresponding compatibility with the  $D\emptyset$  cross-section [12],

$$\sigma_t = 5.3 \pm 1.6 \text{ pb}, \quad (34)$$

is evidently easier to satisfy. It may be noted here that for the higgsino dominated region, the range of  $B_S > 0.45$  and  $\epsilon_3 = 1/4$  would correspond to a suppression factor  $< 1/3$ , in clear conflict with the CDF data.

- iii) The SUSY contribution to the sample of  $\geq 3$  jet events accounts for a fraction

$$2B_S/(3 - B_S) = .22 - .31. \quad (35)$$

This means a 20 – 30% drop in the number of  $t\bar{t}$  events in the dilepton as well as the double  $b$ -tag events compared to the SM prediction if the  $t\bar{t}$  cross-section is normalised to the  $b$ -tagged  $\ell + \geq 3 \text{ jet}$  sample. The present CDF data seems to have  $\sim 8$  events of each kind, of which the 20 – 30% drop is within a  $1\sigma$  effect.

- iv) The SUSY contribution has several kinematic distributions, which are distinct from the SM. Fig. 4 shows the transverse mass distribution of the lepton and the missing  $E_T$

$$M_T = 2E_T^\ell \not{E}_T(1 - \cos \Delta\phi), \quad (36)$$

where the SUSY contribution shows a clear tail beyond the Jacobian peak of the SM contribution. The SM contribution shown corresponds to the  $\geq 3$  jet sample of the CDF  $t\bar{t}$  Monte Carlo including hadronisation and detector resolution effects [25], which are responsible for the spillover to the  $M_T > M_W$  region. In contrast the SUSY contribution corresponds to our parton level MC without these effects, which gives only a conservative estimate of its tail. Nonetheless 30% of the SUSY contribution

is seen to occur at  $M_T > 120 \text{ GeV}$ , in contrast to a 10% spillover for the SM. This corresponds to an excess of

$$.2 \times 2B_S/(3 - B_S) = .044 - .062, \quad (37)$$

i.e. an excess over the SM prediction by about 50%. The present data sample of CDF corresponds to a SM prediction of  $\sim 4$  events with  $M_T > 120 \text{ GeV}$ , of which the 50% excess constitutes a  $1\sigma$  effect. With an order of magnitude increase in the data sample following the main injector run one expects an excess of at least  $3\sigma$ . Similarly the predicted deficit of 20 – 30% in the dilepton and double  $b$ -tag events will each constitute at least a  $2\sigma$  effect. These will provide important tests of the SUSY contribution, since one expects very little background in each case.

### The 90 – 100 GeV Stop Case:

Finally we consider the phenomenological implications of a stop mass of 90 – 100 GeV, which was shown to give a viable contribution to  $R_b$  for the case  $C$ . This is an interesting scenario since it corresponds to a modest  $B_S$  of  $\sim 0.2$ . Besides the stop can undergo charged current decay (24) leading to a soft but visible lepton. The resulting efficiency for the  $E_T^\ell > 20 \text{ GeV}$  cut is  $\sim 1/2$  that of the SM decay. Consequently the overall lepton detection efficiency of the SUSY contribution is  $\sim 3/2$  higher than the previous case. This also implies a somewhat larger efficiency  $\epsilon_3$  for the  $\geq 3$  jet cut compared to the previous case. Taking account of these efficiency factors leads to an overall suppression factor of

$$1 - B_S \simeq 0.8, \quad (38)$$

which is modest compared to (32). Thus the CDF top quark data can accommodate this case more easily.

The most interesting phenomenological test of this scenario follows from the pair production of stops, followed by their leptonic decay (24). This leads to a signal of isolated but relatively soft dilepton events [10]. We have estimated the resulting dilepton signal using our parton level MC with

$$|\eta_\ell| < 1, \quad 20^\circ < \phi_{\ell+\ell^-} < 160^\circ, \quad \cancel{E}_T > 20 \text{ GeV}$$

and

$$E_T^\ell > 10(15) \text{ GeV}. \quad (39)$$

We estimate a signal cross-section of 100(80)  $fb$  for a stop mass of 90 GeV. It should be noted here that this signal has been recently analysed in [26] using the ISAJET program. With the above cuts they estimate a dilepton signal of similar magnitude, which also has an accompanying jet of  $E_T > 15 \text{ GeV}$ . This jet helps to control the  $W^+W^-$  background. Moreover they have used a cut on the scalar sum

$$|E_T^{\ell^+}| + |E_T^{\ell^-}| + |\cancel{E}_T| < 100 \text{ GeV} \quad (40)$$

to suppress the  $t\bar{t}$  as well as the  $W^+W^-$  background without affecting the signal seriously. Thus with the current CDF luminosity of  $0.11 \text{ fb}^{-1}$  one expects  $\sim 10$  soft but isolated

dilepton events for a 90  $GeV$  stop undergoing charged current decay. There is only a modest drop in the signal rate for a stop mass of 100  $GeV$ .

## 4. SUMMARY

The SUSY contributions to  $R_b$  and top quark decay are studied simultaneously over the relevant MSSM parameter space to obtain an optimal solution to the  $R_b$  anomaly within the constraint of the top quark data. Contrary to the popular notion the higgsino dominated region ( $|\mu| \ll M_2$ ) is disfavoured on both counts. It makes a relatively small contribution to  $R_b$  ( $\delta R_b$ ) along with an excessively large one to top  $BR$  ( $B_S$ ). On the other hand one gets a 30% increase in  $\delta R_b$  along with a similar drop in  $B_S$  by going to the mixed region ( $|\mu| \sim M_2$ ), which corresponds to a photino dominated LSP. We have focussed on two points belonging to this region – i.e.  $M_2, \mu = 60, -60 GeV$  and  $40, -70 GeV$ . The latter offers by far the best values of  $\delta R_b$  and  $B_S$ . But it is close to the boundary of the region disallowed by the Tevatron limit on gluino mass, while the former lies safely above the reaches of Tevatron as well as LEP-2. Both give acceptable solutions to the  $R_b$  anomaly for stop mass of 50 – 60  $GeV$ . We analyse the corresponding predictions for top quark decay, which can be tested with Tevatron data. The latter point also gives acceptable solution for a stop mass range of 90 – 100  $GeV$ . In this case one expects a distinctive dilepton signal from the pair production of stop followed by its charged current decay, which can again be tested with the Tevatron data.

## Acknowledgements

This investigation was started as a working group project in WHEPP-IV, Calcutta, last January. We thank the organisers of this workshop for their kind hospitality and Michelangelo Mangano for his participation in the initial stages of this work. The work of MD was supported in part by the US Department of Energy under grant no. DE-FG02-95ER40896, by the Wisconsin Research Committee with funds granted by the Wisconsin Alumni Research Foundation, as well as by a grant from the Deutsche Forschungsgemeinschaft under the Heisenberg program. The work of RMG is partially supported by a grant (No: 3(745)/94/EMR(II)) of the Council of Scientific and Industrial Research, Government of India, while that of SR is partially funded by a project (DO No: SERC/SY/P-08/92) of the Department of Science and Technology, Government of India.

## References

- [1] For a review see H. Haber and G.L. Kane, Phys. Rep. 117, 75 (1985).
- [2] Review of Particle Properties, Phys. Rev. D50, 1173-1826 (1994).
- [3] G. Bhattacharyya, G. Branco and W.S. Hou, NTUTH-95-11 (hep-ph/9512239); E. Ma and D. Ng, hep-ph/9505268; E. Ma, Phys. Rev. D53, 2276 (1996); C.V. Chang, D. Chang and W.Y. Keung, NHCU-HEP-96-1 (hep-ph/9601326); I. Montvay, DESY 96-047.
- [4] P. Chiapetta, J. Leyssac, F.M. Renard and C. Verzegnassi, hep-ph/9601306; G. Altarelli, N. Di Bartolomeo, F. Feruglio, R. Gatto and M. Mangano, hep-ph/9601324; V. Barger, K. Cheung and P. Langacker, MADPH-96-936; K. Agashe, M. Graesser, I. Hinchliffe and M. Suzuki, LBL-38569 (1996).
- [5] LEP Electroweak Working Group Report, LEPEWWG/96-01 (1996).
- [6] M. Boulware and D. Finnell, Phys. Rev. D44, 2054 (1991). The last equation in this paper has a typographic error; the  $C_{11}$  should be  $C_{12}$ .
- [7] J.D. Wells, C. Kolda and G.L. Kane, Phys. Lett. B338, 219 (1994); D. Garcia, R. Jimenez and J. Sola, Phys. Lett. B347, 321 (1995); P.H. Chankowski and S. Pokorski, Phys. Lett. B356, 307 (1995); J. Wells and G.L. Kane, Phys. Rev. Lett. 76, 869 (1996); J. Ellis, J. Lopez and D. Nanopoulos, hep-ph/9512288; E. Ma and D. Ng, hep-ph/9508338; A. Brignole, F. Feruglio and F. Zwirner, hep-ph/9601293.
- [8] P.H. Chankowski and S. Pokorski, IFT-96/6 (hep-ph/9603310).
- [9] G. Passarino and M. Veltman, Nucl. Phys. B160, 151 (1979).
- [10] H. Baer, M. Drees, R.M. Godbole, J.F. Gunion and X. Tata, Phys. Rev. D44, 725 (1991).
- [11] CDF Collaboration: A. Carner, Rencontres de Physique de la Vallee d'Aoste, La Thuile, Italy (1996). J. Huston, Pheno96 Symposium, Madison, Wisconsin, April 1996.
- [12]  $D\bar{D}$  Collaboration: H. Schellman, Pheno96 Symposium, Madison, Wisconsin, April 1996.
- [13] S. Mrenna, C.P. Yuan, Phys. Lett. B367, 188 (1996). These authors favour a stronger bound of  $B_S < 0.25$ .
- [14] ALEPH Collaboration: CERN-PPE/96-10; OPAL Collaboration: CERN-PPE/96-019 and 020.
- [15] One can easily check that in both cases the photino component of  $\tilde{Z}_1$  is 99%.
- [16]  $D\bar{D}$  Collaboration: S. Abachi et. al., Phys. Rev. Lett. 75, 618 (1995); CDF Collaboration: J. Hauser, Proc. 10th Topical Workshop on Proton-Antiproton Collider Physics, Fermilab, May 1995.

- [17] The physical gluino mass is related to the running mass  $M_3(8)$  via the QCD correction factor, i.e.  $m_{\tilde{g}} = M_3[1 + 4.2\alpha_S/\pi]$ . See e.g. N.V. Krasnikov, Phys. Lett. B345, 25 (1995); S.P. Martin and M.T. Vaughn, Phys. Lett. B318, 331 (1993).
- [18]  $D\bar{\theta}$  Collaboration: S. Abachi et. al., Fermilab-pub-95-380-E (Submitted to Phys. Rev. Lett.).
- [19] In this case one also expects a relaxation of the  $B_S$  limit (19) because the stop will undergo charged current decay [20].
- [20] J. Sender, hep-ph/9602354.
- [21] CDF Collaboration: F. Abe et. al., Phys. Rev. Lett. 74, 2626 (1995).
- [22] M. Mangano (private communication).
- [23] E.L. Berger, H. Contopanagos, ANL-HEP-PR-95-85, hep-ph/9512212; S. Catani, M. Mangano, P. Nason, L. Trentadue, CERN-TH/96-21, hep-ph/9602208.
- [24] In practice it suffices to reduce  $m_t$  to 165  $GeV$  when the corresponding reduction in  $B_S$  is taken into account. The drop in  $\delta R_b$  is offset by the rise in  $R_b^{SM}$ .
- [25] CDF Collaboration: F. Abe et. al., Phys. Rev. D50, 2966 (1994).
- [26] H. Baer, J. Sender and X. Tata, Phys. Rev. D50, 4517 (1994).

## Figure Captions

- Fig. 1. SUSY contributions to  $R_b$  (solid) and the top  $BR$  (dashed) are shown as contour plots in stop mass and mixing angle for  $M_2, \mu =$  (a) 150,  $-40$  (b) 60,  $-60$  (c) 40,  $-70$   $GeV$ , with  $\tan \beta = 1.1$ .
- Fig. 2. SUSY contributions to  $R_b$  (dashed) and top  $BR$  (dotted) are shown as contour plots in the  $M_2, \mu$  plane for stop mass of (a) 50 and (b) 60  $GeV$  with  $\theta_{\tilde{t}} = -15^\circ$  and  $\tan \beta = 1.1$ . The  $x$ -axis corresponds to the boundary of the region disallowed by the Tevatron limit ( $m_{\tilde{g}} > 150$   $GeV$ ). Bullets show the parameter choices A,B,C of equation (20).
- Fig. 3. Same as Fig. 2 for  $\tan \beta = 1.4$ . The boundary of the region  $m_{\tilde{t}_1} < M_{\tilde{Z}_1}$  is not shown to avoid overcrowding.
- Fig. 4. The  $(\ell, \cancel{E}_T)$  transverse mass distribution of SM and SUSY contributions to the  $t\bar{t}$  events with free normalisation. The former is taken from the CDF MC of [25] including hadronisation and detector resolution, while the latter is based on our parton level MC result without these effects.

Table I : Chargino and neutralino masses and compositions for three representative points in the  $M_2, \mu$  plane, corresponding to optimal values of  $R_b$  ( $\tan \beta = 1.1$ ).

$M_2, \mu$ (GeV)	$M_{\tilde{W}_i}$ (GeV)	$U_{ij}/V_{ij}$	$M_{\tilde{Z}_i}$ (GeV)	$N_{ij}$
150, -40	70	- .31, .95	40	- .02, .01, .72, .68
		.37, - .92	80	- .25, .31, - .63, .65
	180	.95, .31	85	- .95, - .23, .11, - .15
		.92, .37	181	- .15, .92, .23, - .27
60, -60	97	.31, .95	36	- .92, - .37, .09, - .07
		.95, - .31	60	0, .07, .74, .67
	105	.95, - .31	106	- .28, .83, .28, - .39
		.31, .95	111	- .27, .41, - .61, .63
40, - 70	82	.82, .57	24	- .91, - .40, .06, - .05
		.93, .35	69	- .05, .15, .76, .62
	113	.57, - .82	89	- .31, .79, .21, - .47
		- .35, .93	123	- .26, .42, - .60, .62

Table II : SUSY contributions to  $R_b(\delta R_b)$  and top BR ( $B_s$ ) for the mixed region. The cases satisfying (18) and (19) are ticked as viable solutions to the  $R_b$  anomaly.

$M_2, \mu$ (GeV)	$\tan \beta$	$m_{\tilde{t}_1}$ (GeV)	$\delta R_b$	$B_s$	Remark
60, -60 ( $\theta_{\tilde{t}} = -15^\circ$ )	1.1	60	.0022	.45	
	1.1	50	.0024	.53	
	1.4	50	.0021	.47	
	1.4	60	.0019	.40	✓
40, -70 ( $\theta_{\tilde{t}} = -15^\circ$ )	1.1	60	.0024	.37	✓
	1.1	50	.0026	.46	
	1.4	50	.0023	.41	✓
	1.4	60	.0021	.30	✓
	1.1	90	.0018	.18	✓
( $\theta_{\tilde{t}} = -5^\circ$ )	1.1	90	.0020	.23	✓
	1.1	100	.0018	.16	✓

Table III : Fractional distribution of the SM and SUSY contributions to the  $t\bar{t}$  events in the number of jets. The 4th column shows the numbers of expected  $t\bar{t}$  events in the SM from [11], while the 5th column shows the corresponding numbers of observed (background) events.

$\sigma_n/\sigma$ $n$	SM	SUSY (mixed)	SUSY (higgsino)	No. of CDF events	
				$t\bar{t}$	observed (bg)
1	—	.05	.25	0.8	$70 \pm 9$ ( $69 \pm 11$ )
2	.10	.35	.50	6.4	$45 \pm 7$ ( $28 \pm 4$ )
3	.40	.40	.25	12.8	$18 \pm 4$ ( $6.5 \pm 1$ )
$\geq 4$	.50	.20	—	16.7	$16 \pm 4$ ( $2.6 \pm .5$ )



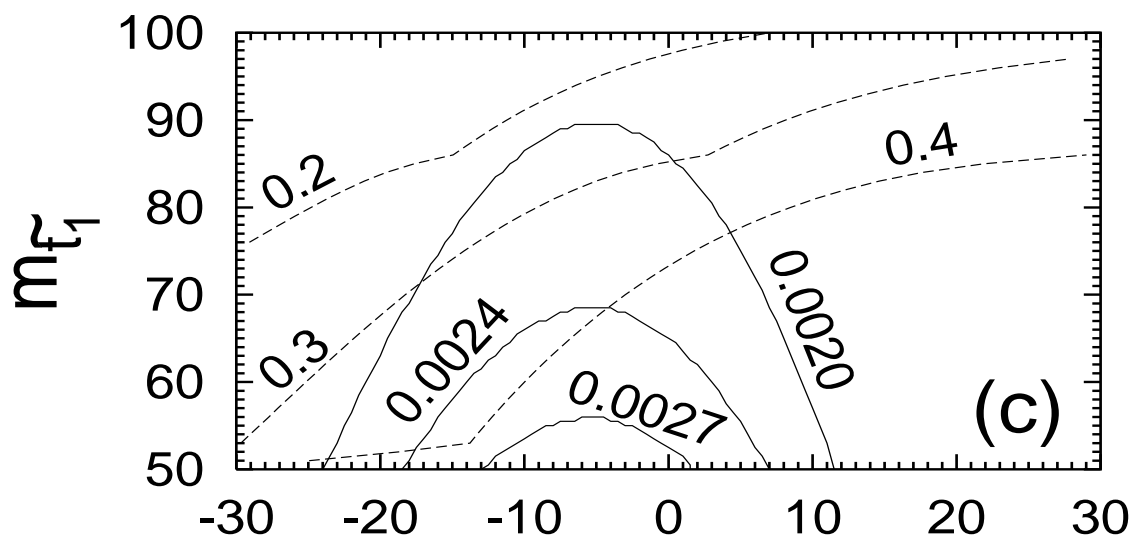
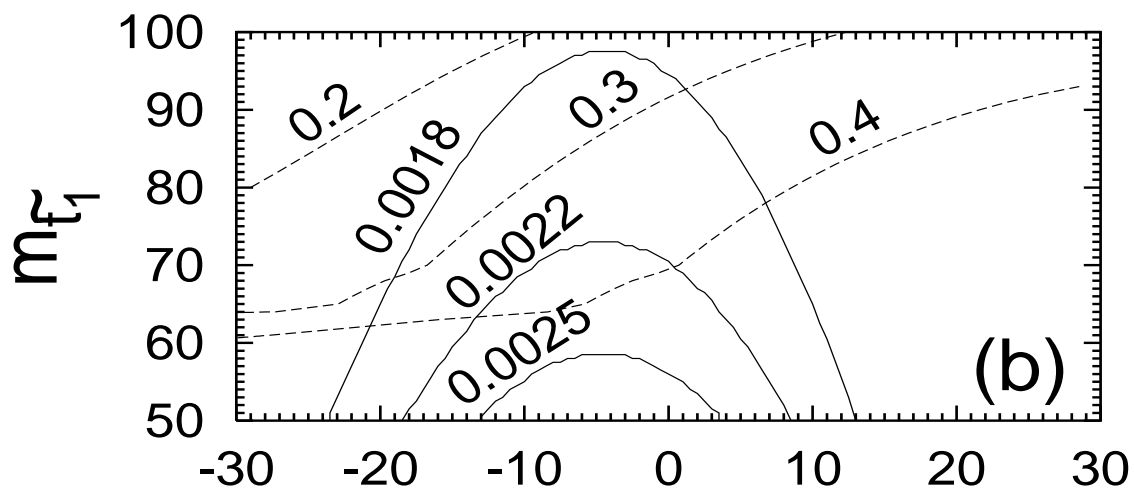
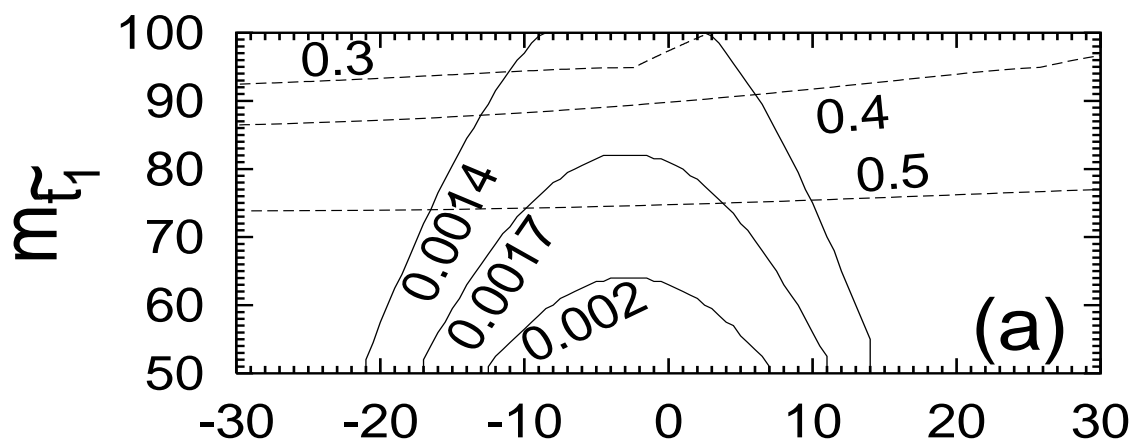


Figure 1

$\theta_{\tau_1}$

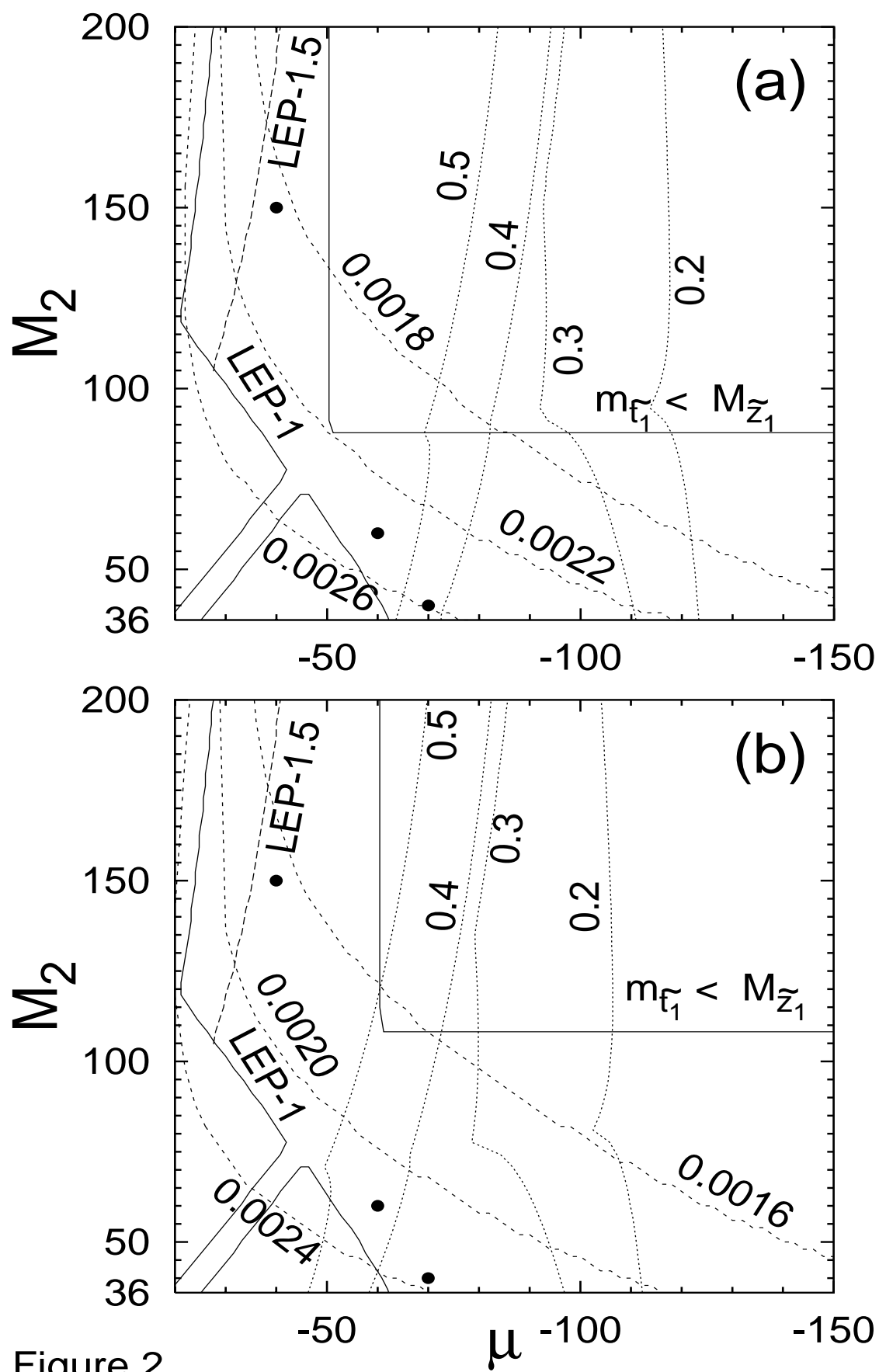


Figure 2

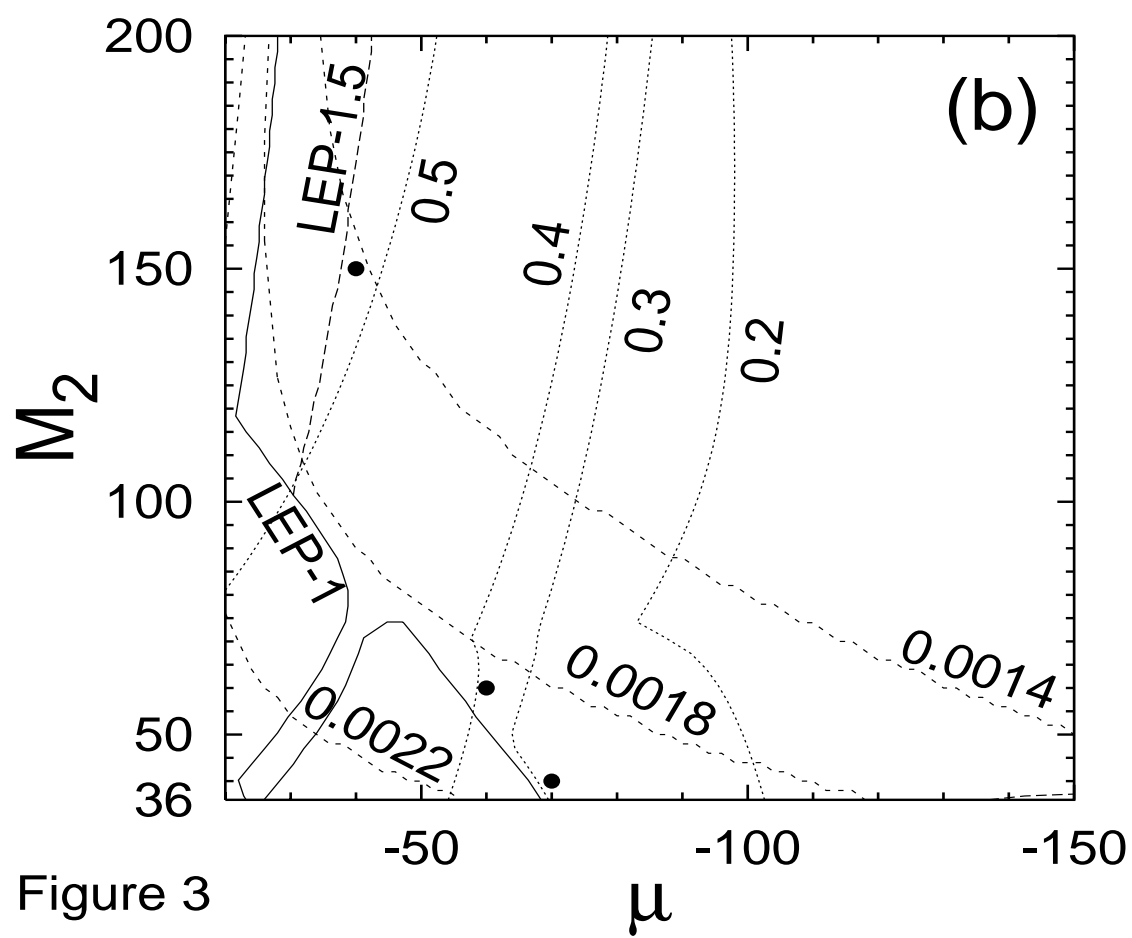
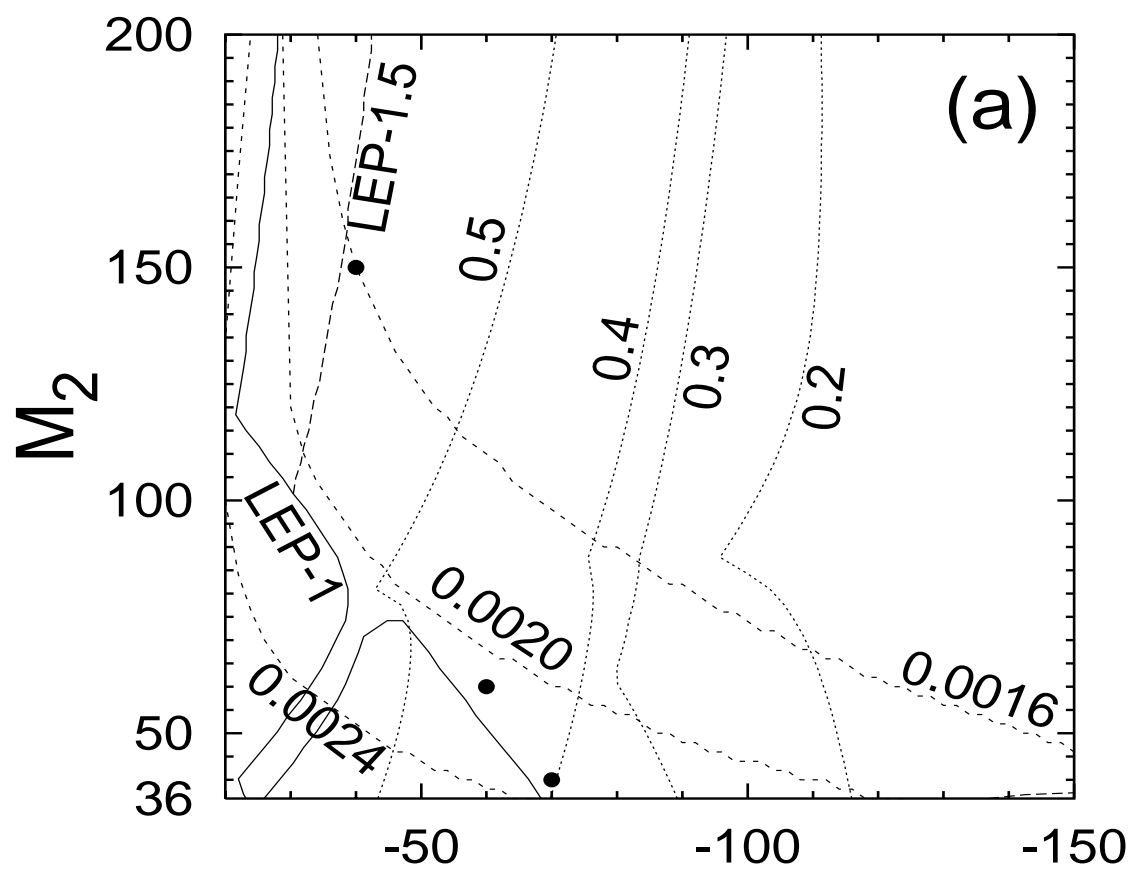


Figure 3

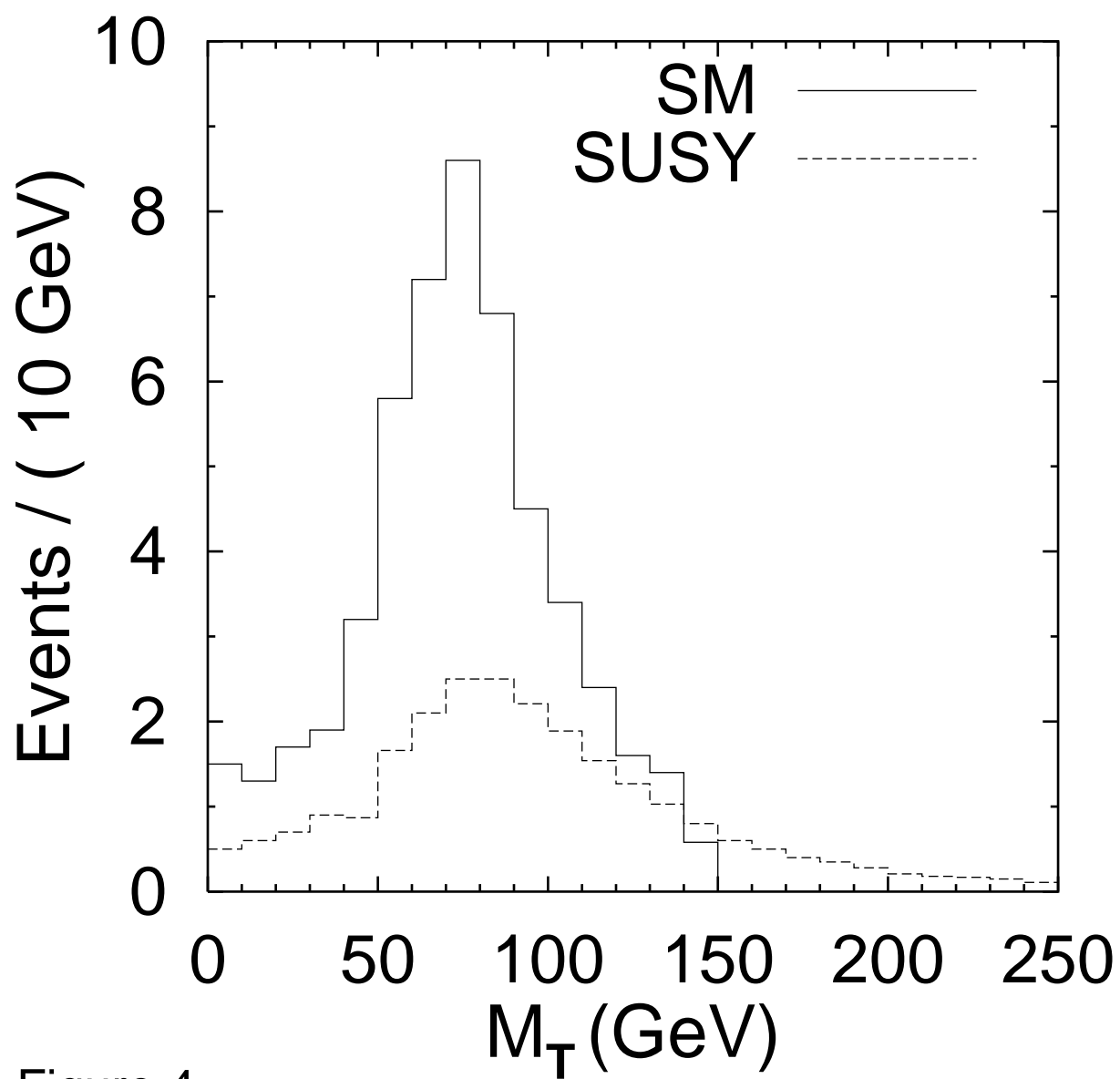


Figure 4